JACS
JOURNAL OF THE AMERICAN CHEMICAL SOCIETY
Article
pubs.acs.org/JACS

Chloride Transport through Supramolecular Barrel-Rosette Ion Channels: Lipophilic Control and Apoptosis-Inducing Activity

Tanmoy Saha,[†] Amitosh Gautam,[†] Arnab Mukherjee,[†] Mayurika Lahiri,[‡] and Pinaki Talukdar*[,†]

[†]Department of Chemistry and [‡]Department of Biology, Indian Institute of Science Education and Research Pune, Dr. Homi Bhabha Road, Pashan, Pune, Maharashtra 411008, India

Supporting Information

ABSTRACT: Despite the great interest in artificial ion channel design, only a small number of channel-forming molecules are currently available for addressing challenging problems, particularly in the biological systems. Recent advances in chloride-mediated cell death, aided by synthetic ion carriers, encouraged us to develop chloride selective supramolecular ion channels. The present work describes vicinal diols, tethered to a rigid 1,3-diethynylbenzene core, as pivotal moieties for the barrel-rosette ion channel formation, and the activity of such channels was tuned by controlling the lipophilicity of designed monomers. Selective transport of chloride ions via an antiport mechanism and channel formation in the lipid bilayer membranes were confirmed for the most active molecule. A theoretical model of the supramolecular barrel-rosette, favored by a network of intermolecular hydrogen bonding, has been proposed. The artificial ion-channel-mediated transport of chloride into cells and subsequent disruption of cellular ionic homeostasis were evident. Perturbation of chloride homeostasis in cells instigates cell death by inducing the caspase-mediated intrinsic pathway of apoptosis.

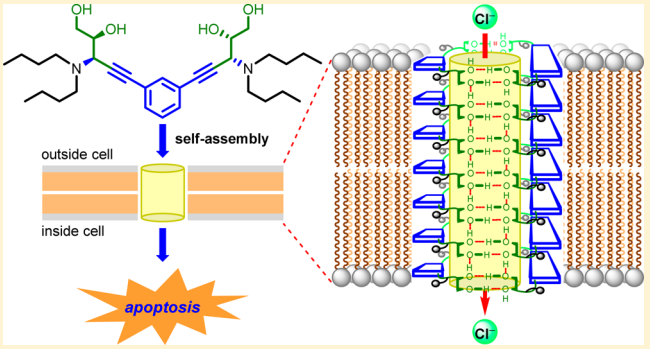

1. INTRODUCTION

Transport of solute molecules across the cellular membrane is extremely crucial to execute fundamental biological processes such as cell to cell communication, energy production, biosynthesis, and metabolism.[1−4] However, the hydrophobic domain of the membrane provides a high thermodynamic barrier which restricts the free movement of all kinds of solutes athwart of the cell.[5] Certain classes of membrane proteins perform the task of controlling exchange of meticulous solutes (such as ions), by overcoming the thermodynamic barrier of the hydrophobic bilayer, to perform the fundamental process of sensory transduction, cell proliferation, and regulation of pH and osmotic pressure.[6−12] Chloride is the most abundant anion in the physiological system. Selective transport of a chloride ion, usually facilitated by chloride selective ion transporters, is pivotal for maintaining a desired potential gradient across the bilayer membranes (e.g., 30−60 mV for eukaryotic cell membranes).[13−15] Diverse biological processes, such as trans-epithelial salt transport, acidification of internal and extracellular compartments, cell volume regulation, cell cycle, and apoptosis[16−18] are related to the selective transport of the ion. However, chloride transport systems are less studied as compared cation transporters.

Malfunction of ion transport proteins or mutation in genes related to chloride transport proteins may lead to various life threatening diseases such as myotonia congenita, cystic fibrosis, Bartter syndrome, Gitelman syndrome, Dent's diseases, renal tubular acidosis, deafness, etc.[19−21] Excess transport of chloride in either lysosomes or late endosomes of cancer cells may impose chemical sequestration of basic chemotherapic drugs, leading to the drug-resistant properties of the cell.[22] Hence, transparent knowledge about the function and workability of chloride transport systems is a burgeoning field for researchers of biochemistry and biotechnology.

Over the years, scientists have shown immense interest in introducing artificial ion transport systems to mimic and better understand natural ion channel functions. The robust chemical nature and adaptable ion transport behavior with the aid of structural manipulation have made artificial ion transport systems a convenient subject of research, compared to their natural congeners. Various strategic designs have been introduced, based on either unimolecular or self-assembled architecture, for the artificial ion channel formation.[23−44] Crown ether based unimolecular hydraphile channels reported by Gokel[27,45] and cyclic peptide based self-assembled ion channels reported by Ghadiri[46] have already promised antibacterial activity against Gram-negative and Gram-positive bacteria. These ion channels undergo a rapid and selective cell death of bacteria by collapsing the transmembrane ion potential by transporting cations. Few crown ether based hydraphile channels, reported by Gokel and Voyer, facilitate cation

Received: October 4, 2016
Published: November 28, 2016

DOI: 10.1021/jacs.6b10379
J. Am. Chem. Soc. 2016, 138, 16443−16451

transport into cells, resulting in the cancer cell death via the necrotic pathway.[47−49] However, apoptotic cell death is preferred for therapeutic development as the necrotic cell death pathway is associated with possibilities of toxicity in the living organs. Recent studies on synthetic chloride ion carriers reveal that selective transport of the ion induces apoptosis in cancer cells by either changing the pH or destroying the ionic homeostasis of cells.[50−55] Therefore, an ion channel, selective for chloride ion transport, can be a judicious choice for apoptosis-inducing cell death studies. Herein, we report a self-assembled barrel-rosette ion channel system constructed by a hydrogen bond network of vicinal diol moieties present at two termini of each monomer. The system portrays tunable ion transport activity achieved by changing the lipophilicity of molecules. These ion channels exhibited Cl^- selective ion transport across lipid membranes, and such transport of Cl^- into the cells triggered the activation of caspase-dependent apoptotic pathways of cell death.

The permeability of ion transport systems in the lipid membranes and, hence, the ion transport property are affected significantly by their lipophilicity. Tuning of ion transport properties based on lipophilicity was extensively studied for ion carriers but was neglected mostly in the synthetic ion channel design.[56−58] Abiding by the lipophilicity−permeability correlation, we designed monomers **1a−1d** for the barrel-rosette ion channel construction (Figure 1A). In each molecule, two vicinal

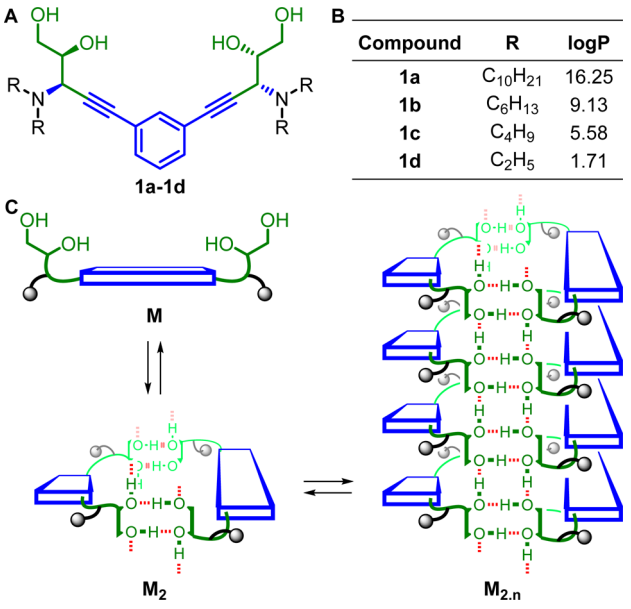

Figure 1. Structure of designed channel-forming molecules **1a−1d** (A); lipophilicity (log*P* values) of channel-forming molecules with different alkyl substitution (B); probable mode of self-assembly of the channel-forming molecules (C).

diol groups were tethered at two alkyne ends of a central rigid 1,3-diethynylbenzene moiety to avoid intramolecular hydrogen bonding interactions and to ensure a definite cavity. According to Lipinski's rule,[59] the log*P* (i.e., partition coefficient in octanol−water) value of 5 is optimum for permeation in the lipid membranes. Therefore, a dialkylamino group was incorporated between each diol and alkyne moiety to vary the amphiphilicity of designed molecules. For monomers **1a−1d**, log*P* values of 16.25, 9.13, 5.53, and 1.71 were calculated using the MarvinSketch program[60] by varying R = $-C_{10}H_{21}$, $-C_6H_{13}$, $-C_4H_9$, and $-C_2H_5$, respectively (Figure 1B). To ensure the stereospecificity around each α-amino alcohol moiety, we planned the synthesis based on our previous report on diastereoselective aldehyde−amine−alkyne three-component (A^3-coupling) reaction.[61,62] The A^3-coupling reaction is also adaptable to the introduction of various $-NR_2$ groups in these molecules. We anticipated, in line with our previous report,[63] that each terminal vicinal diol group of a monomer **M** would participate in hydrogen bonding interactions with a complementary vicinal diol group of a neighboring molecule to form a dimer $\mathbf{M_2}$ as a representative of the cyclic rosette structure (Figure 1C). Accessibility of interlayer hydrogen bonding interactions of consecutive $\mathbf{M_2}$ dimers would lead to a higher-order supramolecular nanotubular architecture $\mathbf{M_{2.n}}$, which upon permeation into the lipid bilayer membrane would form an ion channel. Overall, the nanotubular structure can be viewed as a barrel structure formed by the stacking of dimeric rosettes, providing a hydrophilic path for ion transport. The aliphatic chains at the external surface of the nanotubular architecture would impose additional thermodynamic stability to the channel structure for anchoring it at the hydrophobic layer of the membrane.

2. RESULTS AND DISCUSSION

2.1. Synthesis. The synthesis of compounds **1a−1d** is described in Scheme 1. At first, compound **2** was synthesized

Scheme 1. Synthesis of Derivatives 1a−1d

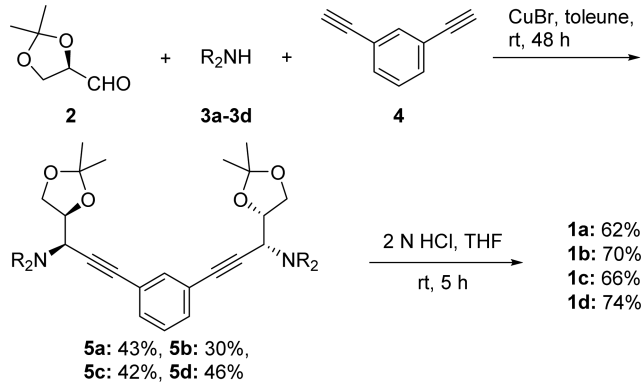

according to the reported procedure.[64] Subsequent multicomponent reaction of (*R*)-(+)-glyceraldehyde acetonide **2** with dialkylamines **3a−3d** and 1,3-diethynylbenzene **4** in the presence of CuBr catalyst gave corresponding bis(acetonide) derivatives **5a−5d**. Acid-catalyzed deportation of terminal acetonides provided final compounds **1a−1d**. All compounds were purified by column chromatography and characterized by ^1H NMR, ^{13}C NMR, HRMS, and IR (see Supporting Information for detailed experiments and characterization).

2.2. Ion Transport Activity of 1a−1d. The ion transport activity of bis(diol) derivatives **1a−1d** across EYPC-LUVs⊃HPTS was recorded by a fluorimetric method. Large unilamellar vesicles (LUVs) were prepared by entrapping the pH-sensitive dye, 8-hydroxypyrene-1,3,6-trisulfonate (HPTS, pK_a = 7.2), and a pH gradient was applied by addition of NaOH (i.e., ΔpH = 0.8) in the extravesicular buffer. The rate of change in the fluorescence intensity was monitored after addition of **1a−1d** separately (Figure S1).[30,31,55,63,65,66]

Measurement of concentration-dependent ion transport activity of compounds **1a−1d** (Figure 2A and Figures S2−

DOI: 10.1021/jacs.6b10379
J. Am. Chem. Soc. 2016, 138, 16443−16451

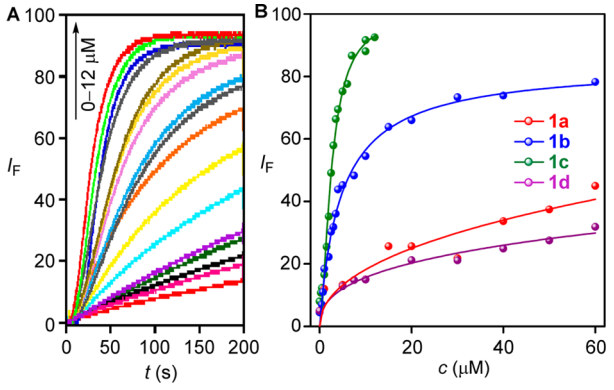

C

Compound	R	logP	EC_{50} (μM)	n
1a	$C_{10}H_{21}$	16.25	38.5 ± 4.9	2.1 ± 0.5
1b	C_6H_{13}	9.13	3.3 ± 0.3	1.7 ± 0.2
1c	C_4H_9	5.58	2.7 ± 0.1	2.4 ± 0.1
1d	C_2H_5	1.71	28.3 ± 4.9	2.2 ± 0.7

Figure 2. Concentration-dependent enhancement of ion transport activity of **1c** (0–12 μM) across EYPC-LUVs⊃HPTS (A). Comparison of dose–response ion transport activity by **1a–1d** (B). Correlation table for calculated log*P* values with determined EC_{50} and Hill coefficient (*n*) values of **1a–1d** (C).

S5) followed by Hill analyses also revealed the activity sequence of **1c** (EC_{50} = 2.7 ± 0.1 μM) > **1b** (EC_{50} = 3.3 ± 0.3 μM) > **1d** (EC_{50} = 28.3 ± 4.9 μM) > **1a** (EC_{50} = 38.5 ± 4.9 μM) (Figures 2C and S2–S5). The maximum activity of **1c** corroborated its optimum lipophilicity (log*P* = 5.58), the optimum among designed bis(diol) derivatives, for efficient translocation of the molecule into the phospholipid bilayer.[59] The decreasing transport activity order **1c** > **1b** ≫ **1a** was associated with the increase in log*P* values upon increasing the length of the alkyl chain, contributing to the poorer aqueous solubility of **1b** and **1a**. The lower activity of **1d**, on the other hand, was the result of a decreased log*P* value, which indicates its higher water solubility compared to that of **1c**. The Hill coefficient, $n \sim 2$, obtained for each compound signified the dimer $\mathbf{M_2}$ as the active rosette structure for the supramolecular nanochannel assembly.

2.3. Ion Selectivity. The pronounced ion transport activity of **1c** prompted us to investigate ion selectivity of this channel-forming molecule. The observed increase of intravesicular pH upon addition of **1c** assumed either via antiport (i.e., either OH^-/A^- or H^+/M^+, where A^- and M^+ are cations and anions) or symport (i.e., either H^+/A^- or M^+/OH^-) process. Therefore, transport activity of **1c** (c = 3 μM) was recorded further by varying either the cation, M^+ (where M^+ = Li^+, Na^+, K^+, Rb^+, and Cs^+), or the anion, A^- (where A^- = F^-, Cl^-, Br^-, I^-, NO_3^-, and ClO_4^-), in the extravesicular buffer to identify the ion selectivity (Figure S6). Variation of cations provided a little difference in the ion transport rate, suggesting the lesser contribution of cations in the transport process (Figure 3A). However, the change of anion resulted in the following activity sequence: $Cl^- \gg Br^- \sim ClO_4^- > F^- \sim NO_3^- > I^-$ (Figure 3B). These studies indicated either OH^-/A^- antiport or H^+/A^- symport as the ion transport mechanism. Equilibration of the applied pH gradient by **1c** in the presence of the selective proton carrier carbonyl cyanide-4-(trifluoromethoxy)-

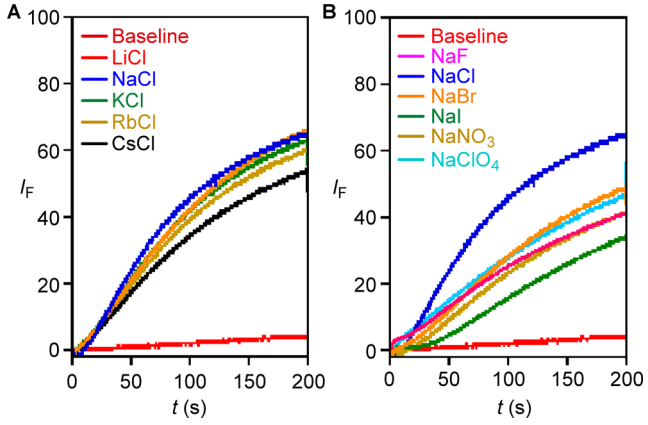

Figure 3. Ion transport activity of **1c** (c = 3 μM) across EYPC-LUVs⊃HPTS determined by varying cations (A) and anions (B) in the extravesicular buffer.

phenylhydrazone (FCCP) was more efficient than that in its absence,[67] indicating the OH^-/A^- antiport as the preferred ion transport mechanism (Figure S7).

2.4. Chloride Ion Transport. Subsequently, the transport of Cl^- by **1b** and **1c** across EYPC-LUVs was studied by monitoring the fluorescence of entrapped lucigenin, a Cl^- selective fluorescent dye.[68] The Cl^-/NO_3^- exchange across LUVs was evaluated by taking $NaNO_3$ and NaCl into intravesicular and extravesicular buffers, respectively (Figure S8). Upon addition of **1c**, a concentration-dependent quenching of fluorescence was observed due to the influx of Cl^- into vesicles (Figure 4A). A similar decrease of fluorescence

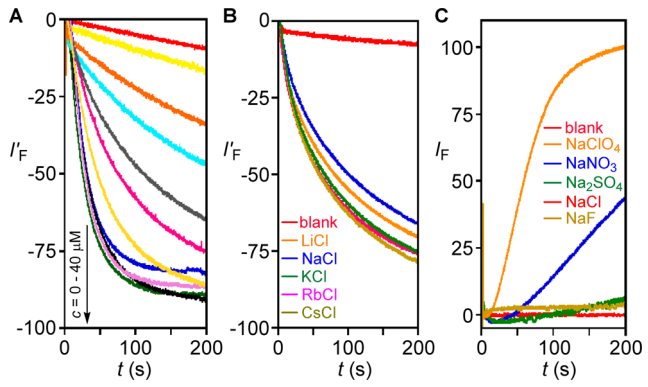

Figure 4. Chloride transport activity of **1c** (0–40 μM) across EYPC-LUVs⊃lucigenin (A). Influx of Cl^- ions across EYPC-LUVs⊃lucigenin upon addition of **1c** (20 μM) with intravesicular $NaNO_3$ and extravesicular MCl (M^+ = Li^+, Na^+, K^+, Rb^+, and Cs^+) (B). Efflux of Cl^- ions across EYPC-LUVs⊃lucigenin upon addition of **1c** (20 μM) with intravesicular NaCl and extravesicular Na_mA salt (A^- = F^-, Cl^-, NO_3^-, SO_4^{2-}, and ClO_4^-; m = valency of an anion) (C).

was observed for **1b**, however, with less activity (Figure S9). Compound **1c** exhibited an initial rate of Cl^-/NO_3^- exchange, which is 66-fold higher than that of **1b** (Table S1).

The cationic composition of the extravesicular buffer was then varied to evaluate the contribution of cations in the Cl^-/NO_3^- exchange (Figure S10). EYPC-LUVs⊃lucigenin were suspended in buffer containing MCl solution (M^+ = Li^+, Na^+, K^+, Rb^+, and Cs^+). No significant difference in the rate of Cl^- influx was encountered, which implies the lack of contribution of cations in the rate-limiting step of the ion transport process

DOI: 10.1021/jacs.6b10379
J. Am. Chem. Soc. 2016, 138, 16443–16451

(Figure 4B). Further, the anionic composition in the extravesicular buffer was varied as Na_mA (A^- = F^-, ClO_4^-, NO_3^-, SO_4^{2-}, Cl^-; m = valency of an anion) by keeping NaCl as the intravesicular salt (Figure S11). A remarkable difference in the rate of Cl^- efflux was observed, which ascertains the involvement of the extravesicular anions in the rate of transport of Cl^- by the antiport mechanism (Figure 4C). The antiport mechanism was further confirmed by using valinomycin (V), a K^+ selective transporter, in the extravesicular buffer (Figure S12).[55] KCl solution was added in the extravesicular buffer of EYPC-LUVs⊃lucigenin, keeping intravesicular $NaNO_3$, and rate of influx of Cl^- by **1c** (20 μM) was examined in the absence and the presence of valinomycin (2 μM). The synergistic effect of Cl^- influx by **1c** and K^+ influx by valinomycin was evident from the acceleration of the Cl^- transport rate, which was further quantified (Figure S13). The enhanced rate of Cl^- transport in the presence of valinomycin established the Cl^-/NO_3^- antiport as the preferred transport mechanism involving **1c**.

2.5. Evidence of Ion Channel Formation. To appraise the necessary evidence for ion channel formation by the most active compound **1c**, we measured electrical conductance across planar lipid bilayer membrane. The planar lipid bilayer, consisting of 1,2-diphytanoyl-*sn*-glycero-3-phosphocholine (DPhPC) lipid, was prepared over the orifice connecting two electrolyte chambers of the instrument. Electrical conductance between two chambers, after applying a voltage, provides information about ion channel formation.[32] Significant conduction of ions was observed by adding **1c** (c = 80 μM) in the cis chamber of the electrolyte solution. The periodic opening and closing events were also observed at different holding potentials, corroborating the ion channel formation at the planar bilayer by **1c** (Figure 5). The single-channel conductance G = 79.7 ± 4.9 pS and the diameter d = 4.71 ± 0.16 Å were calculated for the supramolecular ion channel formed by **1c**.

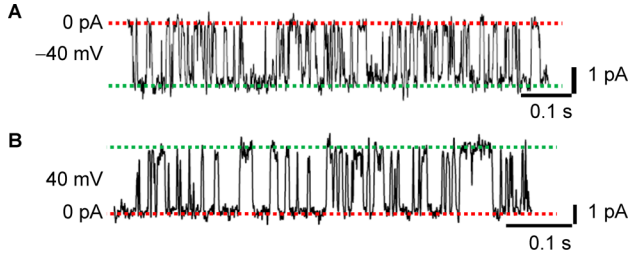

Figure 5. Single-channel current traces recorded at −40 mV (A) and +40 mV (B), holding potentials in 1 M symmetrical KCl solution. The baseline current is indicated by 0 pA at the right-hand side. The main conductance state is indicated by two dotted lines.

2.6. Molecular Modeling of the Ion Channel. To understand the molecular picture of the nanochannel, we have proposed a model based on the hydrogen bonding network of the bis(diol) system. Alkyl chains were truncated to ethyl for simplicity in the calculation. Semiempirical quantum calculations were performed to obtain molecular level insight of the supramolecular architecture. At first, the face-to-face dimeric unit was optimized using Gaussian 09[69] software with wB97XD[70] functional and 6-31G(d,p) basis set to obtain the rosette structure $\mathbf{M_2}$ (Figure S15). The nanotubular structure was achieved by placing five optimized rosette units on top of each other. This oligomeric assembly was further optimized with MOPAC2012[71] software using the PM6-DH+[72] method, and the result indicates the formation of the nanochannel $\mathbf{M_{2.5}}$ with the hydrophilic interior and hydrophobic exterior, in line with our proposition (Figures 6 and S16). We calculated the

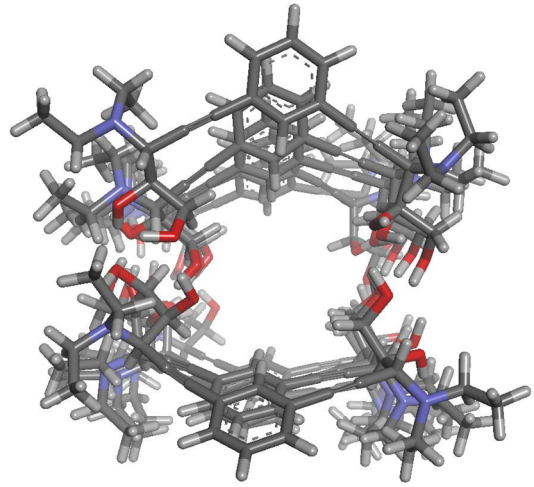

Figure 6. Top view of the optimized structures of ion channel **1d**. Compound **1d** was selected for the optimization for simplicity of the calculation, due to the presence of fewer atoms in this structure of **1d** than in others.

average diameter using the radius of gyration method for the middle layer. The diameter is found to be 6.4 Å. However, the cavity is not circular, giving us different values for major (8.4 Å) and minor (3.8 Å) axes, as shown in Figure S17. The experimental value (4.7 Å), based on the conductance measurement, is understandably close to the smaller value, that is, the minor axis value.

2.7. Effect of Ion Transport in Biological Systems. Formation of an efficient artificial ion channel in spherical as well as in planar lipid bilayers prompted us to investigate the ion transport activity of **1c** across the cell membrane. The change in Cl^- concentration in the intracellular matrix was monitored with a cell-permeable chloride selective dye *N*-(ethoxycarbonylmethyl)-6-methoxyquinolinium bromide (MQAE).[73,74] A significant amount of quenching of the fluorescence intensity of MQAE (λ_{ex} = 350 nm and λ_{em} = 460 nm) was encountered upon preincubation of HeLa cells with **1c** in a concentration-dependent manner (Figure 7). The

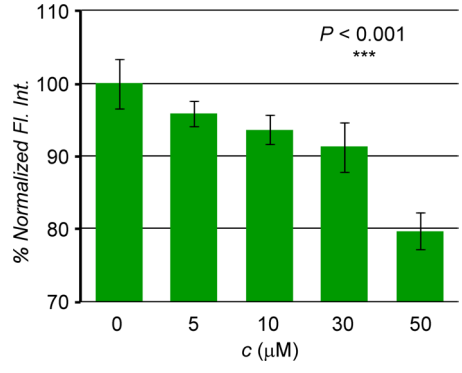

Figure 7. Normalized fluorescence intensity of HeLa cells incubated with MQAE (5 mM) for 3 h followed by treatment of **1c** (0−50 μM) for 24 h.

DOI: 10.1021/jacs.6b10379
J. Am. Chem. Soc. 2016, 138, 16443−16451

dose-dependent quenching of fluorescence implies the enhanced chloride concentration at the intracellular matrix, transported through an artificial ion channel made up of **1c**.

The successful Cl^- transports across the cell membrane prompted us to investigate the impact of Cl^- transport in cell viability. According to a few recent studies, the stimulated transport of Cl^- can induce apoptosis via disruption of ionic homeostasis of the cell.[53,55,75,76] At first, the effect of **1c** in cell viability was screened in various cancer (e.g., lung adenocarcinoma epithelial A549, human cervical cancer HeLa, human breast cancer MCF7, and human bone osteosarcoma U2OS) and normal (e.g., mouse fibroblast NIH3T3) cell lines of different origin. A single-point screening of cell viability was done by MTT assay after incubation of **1c** (10 μM) with different cell lines. A considerable amount of cell death was observed upon treatment of **1c** irrespective of cell type and origin (Figure 8).

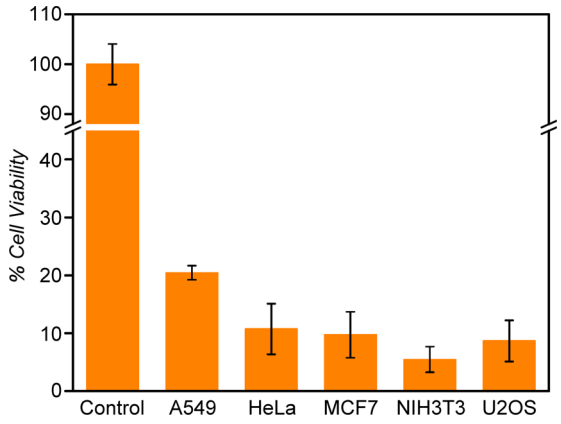

Figure 8. Cell viability obtained from single-point screening of compounds **1c** (10 μM each) by MTT assay. Cell viability was checked after 24 h treatment of **1c** in various cell lines: from left to right, A549, HeLa, MCF7, NIH3T3, and U2OS.

The Cl^--transport-mediated cell death, via the artificial ion channel, was confirmed by subsequent comparison of the cell viability in the presence and the absence of Cl^- ions in the extracellular media. Two different varieties of HBSS (Hanks balanced salt solution) were prepared, with and without Cl^- ions, to be used as extracellular media. The HeLa cells were suspended in two different types of HBSS media, separately, and incubated with **1c** at various concentrations. Cell viability observed for cells suspended in the Cl^--free HBSS media was significantly higher than that of the Cl^- ion containing buffer (Figure 9). The difference in cell viability in the presence and the absence of Cl^- ions clearly indicates that the cell death is due to the enhanced level of Cl^- ions in the intracellular matrix, transported through an artificial ion channel formed by **1c**.

A detailed study has been carried out to evaluate the mode of Cl^- ion-transport-mediated cell death via either apoptosis or necrosis. In the intrinsic pathway of apoptosis, disruption of mitochondrial membrane potential (MMP) may lead to the release of cytochrome *c* from the intra-mitochondrial space to the cytoplasm, which subsequently binds with *Apaf*-1 and procaspase 9 to form apoptosome.[77] Release of cleaved caspase 9 from apoptosome triggers the expression of cleaved caspase 3, known to be the executioner caspase, which subsequently undergoes a few consecutive processes to induce apoptosis of the cell.[78−81] At first, the change in mitochondrial membrane

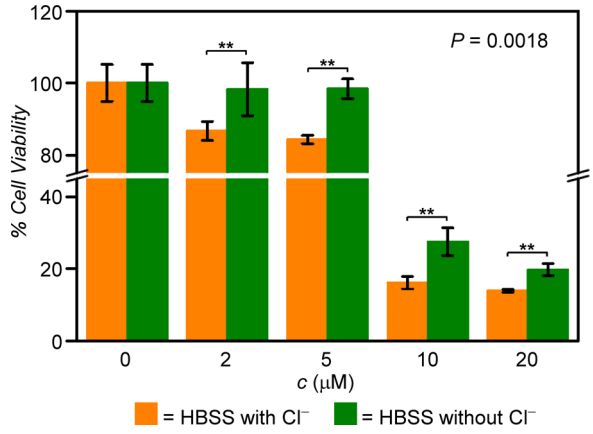

Figure 9. MTT assay comparing cell viability of HeLa cells in the presence and the absence of Cl^- ions in extracellular media (HBSS buffer) upon dose-dependent treatment of **1c** (0−20 μM) for 24 h.

potential, as the indication of early stages of apoptosis, was monitored with an MMP-sensitive probe JC-1. This dye exhibits red fluorescence emission because of *J*-aggregation in the healthy mitochondrial membrane, while depolarization of the mitochondrial membrane leads to dispersion of the dye in cytosol, resulting green fluorescence emission.[82,83] Preincubation of HeLa cells with **1c** (0, 5, 10, and 20 μM) followed by treatment with JC-1 dye resulted in the stepwise dose-dependent decrease of red fluorescence with the concurrent increase in green fluorescence (Figure 10A−D). The

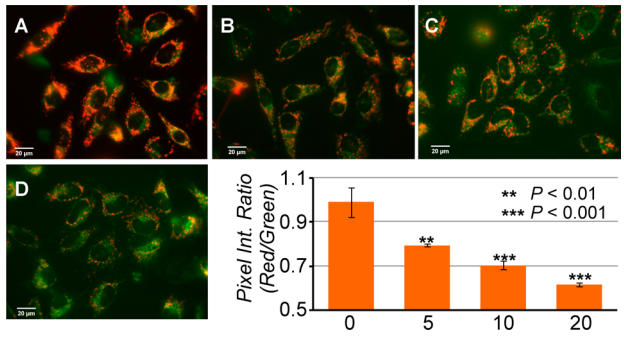

Figure 10. Live cell imaging of HeLa cells upon treatment with 0 μM (A), 5 μM (B), 10 μM (C), and 20 μM (D) of **1c** for 24 h followed by staining with JC-1 dye. Red and green channel images were merged to generate the displayed image. The pixel ratio (red/green) for each set of cells was plotted in the bar graph (E).

quantification of the pixel intensity ratio (red/green) also suggested that the change in fluorescence is an upshot of the mitochondrial membrane depolarization (Figure 10E). The disruption of the ionic homeostasis of cells, due to the excess transport of Cl^- ion through the artificial anion channels, is, therefore, responsible for the change in the membrane potential of mitochondria.

The change in ionic homeostasis of cells also causes an interruption of the electron transport chain in the mitochondrial respiratory cycles, resulting in the abnormal reactive oxygen species (ROS) production.[84,85] A concentration-dependent enhancement of ROS level was encountered when HeLa cells were incubated with **1c** (0−50 μM) followed by incubation with 3-methyl-7-(4,4,5,5-tetramethyl-1,3,2-dioxabor-

DOI: 10.1021/jacs.6b10379
J. Am. Chem. Soc. 2016, 138, 16443−16451

olan-2-yl)-2*H*-chromen-2-one, a ROS-sensitive probe (Figure 11).

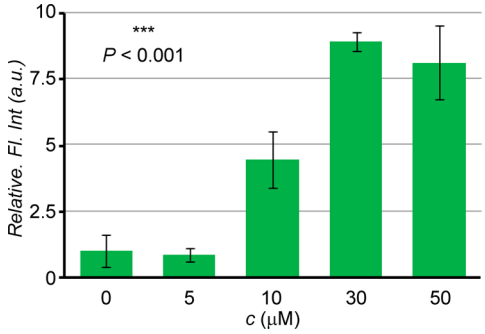

Figure 11. Measurement of ROS production in HeLa cells upon incubation with different concentrations of **1c** (0–50 μM) for 7 h, followed by treatment with the ROS probe (100 μM) for 1 h. Fluorescence intensities were recorded using a plate reader at λ_{em} = 460 nm (λ_{ex} = 315 nm) and normalized with respect to the emission intensity of untreated cells.

Cytochrome *c*, a well-conserved electron transport protein, is a part of the respiratory chain and localized between mitochondrial intermembrane spaces. Release of cytochrome *c* upon apoptotic stimulation may lead to caspase-dependent apoptotic pathways.[86−88] The elevated level of ROS can trigger the opening of the mitochondrial permeability transition pore (PTP), mainly formed by natural ion channels present in the mitochondrial membrane, resulting in the disruption of the outer-mitochondrial membrane and subsequent release of cytochrome *c* into the cytosol.[89−91] On the other hand, enhanced amounts of ROS may downregulate the Bcl-2 and Bcl-xL proteins, resulting in the opening of mitochondrial PTP.[89,92,93] Therefore, the release of cytochrome *c* was monitored by immunostaining with a specific antibody. A considerable amount of enhancement on fluorescence intensity and dispersion of the fluorescence signal all over the cytosol was detected upon treatment of **1c** (0, 10, and 20 μM) in HeLa cells for 8 h (Figure 12), which signifies the release of cytochrome *c* from mitochondria, confirmed by the change in ionic homeostasis.

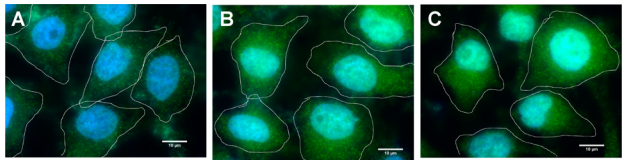

Figure 12. HeLa cells treated first with 0 μM (A), 10 μM (B), and 20 μM (C) of **1c** for 8 h and then fixed and analyzed for cytochrome *c* release by immunostaing with cytochrome *c* specific primary antibody. Nuclei were stained with Hoechst 33342. Cell boundaries were marked manually for better clarity.

The released cytochrome *c* can initiate the program of apoptotic cell death by provoking a family of caspases.[80,94−96] In next stage, the expression of the caspase family was investigated for the proper understanding of the pathway of mitochondria-dependent apoptosis. The levels of cleaved caspase 9 and caspase 3 were examined by immunoblot analysis. A significant amount of enhancement in the amount of cleaved caspase 9 and cleaved caspase 3 was observed upon incubation with increasing concentration of **1c** (0–20 μM). The enhancements in the levels of caspases were quantified with respect to the GAPDH level (Figure S19). The expression of caspase 9 and caspase 3 confirms the caspase-mediated intrinsic pathway of apoptosis as the pathway of cell death (Figure 13). In addition to that, cleavage of poly(ADP-ribose)

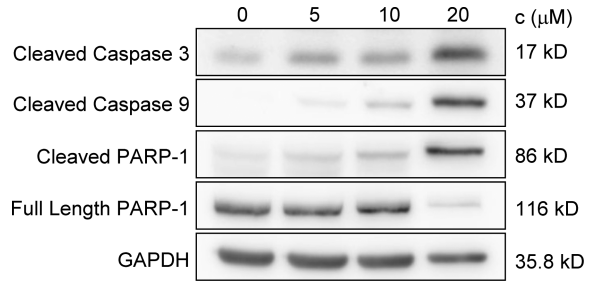

Figure 13. Immunoblot assay for cleaved caspase 9, caspase 3, and PARP-1 in HeLa cells, after 24 h incubation with various concentrations (0, 5, 10, and 20 μM) of **1c**. Data were quantified with respect to glyceraldehyde 3-phosphate dehydrogenase (GAPDH) levels.

polymerase (PARP) by endogenous caspases is a well-known phenomenon during apoptosis.[97,98] Cleavage of PARP-1 prevents the futile repair of DNA strand breaks to facilitate the apoptotic process.[97,99] A significant amount of degradation of full-length PARP-1 (116 kDa) with a concomitant increase of cleaved PARP-1 (86 kDa) was encountered upon immunoblot analysis of HeLa cells incubated with various concentrations of **1c** (0–20 μM). The activation of cleaved PARP-1 epitomizes an additional validation of **1c**-mediated caspase-dependent apoptosis (Figure 13). On the other hand, phosphorylation of the Ser-15 position of p53 protein is a well-known pathway of the p53-mediated apoptosis program.[100,101] No phosphorylation step was found on Ser-15 of the p53 protein, which abolishes the possibility of a p53-mediated apoptosis program (Figure S20).

To explicate the intrinsic pathway of apoptosis as the prime mode of cell death, the cell viability was checked in the presence of caspase inhibitors. Benzyloxycarbonyl-Asp(OMe)-Glu(OMe)-Val-Asp(OMe)-fluoromethylketone (z-DEVD-fmk) and benzyloxycarbonyl-Leu-Glu(OMe)-His-Asp(OMe)-fluoromethylketone (z-LEHD-fmk) are small cell-permeable peptides, known to have an inhibitory action for expression of cleaved caspase 3 and caspase 9, respectively.[95,102,103] The **1c**-mediated caspase-dependent apoptosis can be inhibited by introduction of caspase inhibitors. An extremely significant amount of retention of cell viability was detected upon preincubation of HeLa cells with z-DEVD-fmk and z-LEHD-fmk followed by treatment of **1c** (Figure 14). Restoring of cell viability, due to inhibition of the executioner caspase, strongly supports the prime mode of cell death via the caspase-mediated intrinsic pathway of apoptosis.

3. CONCLUSION

In summary, we have introduced small bis(diol) molecules for the strategic construction of a supramolecular nanotubular assembly that allows selective transmembrane transport of chloride ions. Formation of the nanotubular structure was achieved by intermolecular hydrogen bonding interactions from the hydroxyl moieties present at two termini of a molecule. The molecular library of these bis(diol)s was designed by varying

DOI: 10.1021/jacs.6b10379
J. Am. Chem. Soc. 2016, 138, 16443−16451

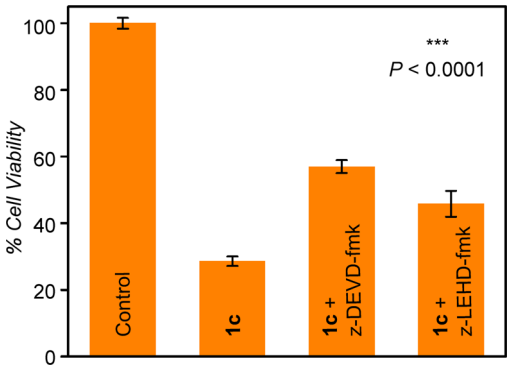

Figure 14. HeLa cells were preincubated with z-DEVD-fmk or z-LEHD-fmk (100 μM each) for 3 h followed by incubation with **1c** (20 μM) for 24 h.

their log*P* values. These compounds were synthesized following the Cu(I)-catalyzed aldehyde−amine−alkyne three-component reaction followed by acid-catalyzed ketal deprotection chemistry to obtain free hydroxyl groups. Ion transport across vesicles revealed an excellent alliance of log*P* value with the transport activity, correlating Lipinski's rule of lipid membrane permeability. The bis(diol) system favored anion transport with prominent chloride ion selectivity, and the antiport mechanism for the anion transport was established. The transmembrane ion transport process was also operative through an ion channel constructed from the self-assembly of bis(diol) molecules, and a computational model for such a supramolecular channel was also established.

The bis(diol) system was efficient at delivering Cl^- ions into cells indicated by the increase in the intracellular Cl^- ion level, and the process also resulted in significant cell death. Change in the mitochondrial membrane potential, subsequent generation of excess ROS, and release of cytochrome *c* from mitochondrial intermembrane spaces were encountered upon disruption of the Cl^- ion homeostasis. The observed cell death was a consequence of the apoptosis process, as evident from the expression of proteins of the caspase family, namely, caspase 3 and caspase 9. The caspase-mediated apoptosis pathway was further confirmed by monitoring the diminution of ion-transport-mediated cell death in the presence of caspase inhibitors. Hence, artificial Cl^- channels displaying apoptosis-inducing activity can be a potential tool for therapeutic treatment in the future.

■ ASSOCIATED CONTENT

Supporting Information

The Supporting Information is available free of charge on the ACS Publications website at DOI: 10.1021/jacs.6b10379.

Experimental procedures, compound characterization data, theoretical calculations, and biological evaluation and data (PDF)

■ AUTHOR INFORMATION

Corresponding Author

*ptalukdar@iiserpune.ac.in

ORCID

Arnab Mukherjee: 0000-0001-5691-6120

Pinaki Talukdar: 0000-0003-3951-4335

Notes

The authors declare no competing financial interest.

■ ACKNOWLEDGMENTS

This work was supported in part by collaborative grants from SERB, DST, Govt. of India (Grant Nos. EMR/2014//000873B and EMR/2016/001069). M.L. was supported through the Department of Biotechnology, Govt. of India (BT/PR8699/MED/30/1018/2013). T.S. thanks UGC (University Grant Commission), India, for research fellowships. We also thank Ms. Libi Anandi, Ms. Vaishali Chakaborty, Mr. Satish Bodakuntla, Mr. Ashiq K.A. and Mr. Abhik Mallick of IISER Pune, and Gilman Toombes of NIH, USA for their valuable discussions. This work is dedicated to Prof. K.N. Ganesh.

■ REFERENCES

(1) Stein, W. D. *Channels, Carriers, and Pumps: An Introduction to Membrane Transport*; Academic Press: San Diego, CA, 1990.
(2) Hladky, S. B.; Haydon, D. A. Ion Movement in Gramicidin Channels. In *Current Topics in Membranes and Transport*; Bronner, F., Ed.; Academic Press: New York, 1984; Vol. *21*, pp 327−372.
(3) Agre, P. *Angew. Chem., Int. Ed.* **2004**, *43*, 4278.
(4) Hille, B. *Ion Channels of Excitable Membranes*, 3rd ed.; Sinauer Associates: Sunderland, MA, 2001.
(5) Diamond, J. M.; Wright, E. M. *Annu. Rev. Physiol.* **1969**, *31*, 581.
(6) Allen, T. W.; Andersen, O. S.; Roux, B. *Proc. Natl. Acad. Sci. U. S. A.* **2004**, *101*, 117.
(7) MacKinnon, R. *Angew. Chem., Int. Ed.* **2004**, *43*, 4265.
(8) Doyle, D. A.; Cabral, J. M.; Pfuetzner, R. A.; Kuo, A.; Gulbis, J. M.; Cohen, S. L.; Chait, B. T.; MacKinnon, R. *Science* **1998**, *280*, 69.
(9) Bayrhuber, M.; Meins, T.; Habeck, M.; Becker, S.; Giller, K.; Villinger, S.; Vonrhein, C.; Griesinger, C.; Zweckstetter, M.; Zeth, K. *Proc. Natl. Acad. Sci. U. S. A.* **2008**, *105*, 15370.
(10) Stark, G.; Ketterer, B.; Benz, R.; Läuger, P. *Biophys. J.* **1971**, *11*, 981.
(11) Chiu, S. Y.; Wilson, G. F. *J. Physiol.* **1989**, *408*, 199.
(12) DeCoursey, T. E.; Chandy, K. G.; Gupta, S.; Cahalan, M. D. *Nature* **1984**, *307*, 465.
(13) Santacroce, P. V.; Davis, J. T.; Light, M. E.; Gale, P. A.; Iglesias-Sanchez, J. C.; Prados, P.; Quesada, R. *J. Am. Chem. Soc.* **2007**, *129*, 1886.
(14) Jentsch, T. J.; Stein, V.; Weinreich, F.; Zdebik, A. A. *Physiol. Rev.* **2002**, *82*, 503.
(15) Duran, C.; Thompson, C. H.; Xiao, Q.; Hartzell, H. C. *Annu. Rev. Physiol.* **2010**, *72*, 95.
(16) Hong, S.; Bi, M.; Wang, L.; Kang, Z.; Ling, L.; Zhao, C. *Oncol. Rep.* **2015**, *33*, 507.
(17) Benz, R.; Hancock, R. E. W. *J. Gen. Physiol.* **1987**, *89*, 275.
(18) Lange, K. *J. Cell. Physiol.* **2000**, *185*, 21.
(19) Vaughan-Jones, R. D.; Spitzer, K. W.; Swietach, P. *J. Mol. Cell. Cardiol.* **2009**, *46*, 318.
(20) Jentsch, T. J.; Maritzen, T.; Zdebik, A. A. *J. Clin. Invest.* **2005**, *115*, 2039.
(21) Choi, J. Y.; Muallem, D.; Kiselyov, K.; Lee, M. G.; Thomas, P. J.; Muallem, S. *Nature* **2001**, *410*, 94.
(22) Su, J.; Xu, Y.; Zhou, L.; Yu, H.-M.; Kang, J.-S.; Liu, N.; Quan, C.-S.; Sun, L.-K. *Anat. Rec.* **2013**, *296*, 595.
(23) Pregel, M. J.; Jullien, L.; Canceill, J.; Lacombe, L.; Lehn, J.-M. *J. Chem. Soc., Perkin Trans. 2* **1995**, 417.
(24) Qi, Z.; Sokabe, M.; Donowaki, K.; Ishida, H. *Biophys. J.* **1999**, *76*, 631.
(25) Murillo, O.; Suzuki, I.; Abel, E.; Murray, C. L.; Meadows, E. S.; Jin, T.; Gokel, G. W. *J. Am. Chem. Soc.* **1997**, *119*, 5540.
(26) Sakai, N.; Brennan, K. C.; Weiss, L. A.; Matile, S. *J. Am. Chem. Soc.* **1997**, *119*, 8726.
(27) Leevy, W. M.; Donato, G. M.; Ferdani, R.; Goldman, W. E.; Schlesinger, P. H.; Gokel, G. W. *J. Am. Chem. Soc.* **2002**, *124*, 9022.
(28) Sidorov, V.; Kotch, F. W.; Abdrakhmanova, G.; Mizani, R.; Fettinger, J. C.; Davis, J. T. *J. Am. Chem. Soc.* **2002**, *124*, 2267.

(29) Madhavan, N.; Robert, E. C.; Gin, M. S. *Angew. Chem., Int. Ed.* **2005**, *44*, 7584.
(30) Talukdar, P.; Bollot, G.; Mareda, J.; Sakai, N.; Matile, S. *J. Am. Chem. Soc.* **2005**, *127*, 6528.
(31) Gorteau, V.; Bollot, G.; Mareda, J.; Perez-Velasco, A.; Matile, S. *J. Am. Chem. Soc.* **2006**, *128*, 14788.
(32) Ishida, H.; Qi, Z.; Sokabe, M.; Donowaki, K.; Inoue, Y. *J. Org. Chem.* **2001**, *66*, 2978.
(33) Wilson, C. P.; Webb, S. J. *Chem. Commun.* **2008**, 4007.
(34) Moszynski, J. M.; Fyles, T. M. *J. Am. Chem. Soc.* **2012**, *134*, 15937.
(35) Muraoka, T.; Shima, T.; Hamada, T.; Morita, M.; Takagi, M.; Tabata, K. V.; Noji, H.; Kinbara, K. *J. Am. Chem. Soc.* **2012**, *134*, 19788.
(36) Langecker, M.; Arnaut, V.; Martin, T. G.; List, J.; Renner, S.; Mayer, M.; Dietz, H.; Simmel, F. C. *Science* **2012**, *338*, 932.
(37) Dambenieks, A. K.; Vu, P. H. Q.; Fyles, T. M. *Chem. Sci.* **2014**, *5*, 3396.
(38) Barboiu, M.; Le Duc, Y.; Gilles, A.; Cazade, P.-A.; Michau, M.; Marie Legrand, Y.; van der Lee, A.; Coasne, B.; Parvizi, P.; Post, J.; Fyles, T. *Nat. Commun.* **2014**, *5*, 4142.
(39) Xin, P.; Zhu, P.; Su, P.; Hou, J.-L.; Li, Z.-T. *J. Am. Chem. Soc.* **2014**, *136*, 13078.
(40) Muraoka, T.; Endo, T.; Tabata, K. V.; Noji, H.; Nagatoishi, S.; Tsumoto, K.; Li, R.; Kinbara, K. *J. Am. Chem. Soc.* **2014**, *136*, 15584.
(41) Gilles, A.; Barboiu, M. *J. Am. Chem. Soc.* **2016**, *138*, 426.
(42) Das, R. N.; Kumar, Y. P.; Schütte, O. M.; Steinem, C.; Dash, J. *J. Am. Chem. Soc.* **2015**, *137*, 34.
(43) Wei, X.; Zhang, G.; Shen, Y.; Zhong, Y.; Liu, R.; Yang, N.; Al-mkhaizim, F. Y.; Kline, M. A.; He, L.; Li, M.; Lu, Z.-L.; Shao, Z.; Gong, B. *J. Am. Chem. Soc.* **2016**, *138*, 2749.
(44) Basak, D.; Sridhar, S.; Bera, A. K.; Madhavan, N. *Org. Biomol. Chem.* **2016**, *14*, 4712.
(45) Leevy, W. M.; Gokel, M. R.; Hughes-Strange, G. B.; Schlesinger, P. H.; Gokel, G. W. *New J. Chem.* **2005**, *29*, 205.
(46) Fernandez-Lopez, S.; Kim, H.-S.; Choi, E. C.; Delgado, M.; Granja, J. R.; Khasanov, A.; Kraehenbuehl, K.; Long, G.; Weinberger, D. A.; Wilcoxen, K. M.; Ghadiri, M. R. *Nature* **2001**, *414*, 329.
(47) Leevy, W. M.; Gammon, S. T.; Levchenko, T.; Daranciang, D. D.; Murillo, O.; Torchilin, V.; Piwnica-Worms, D.; Huettner, J. E.; Gokel, G. W. *Org. Biomol. Chem.* **2005**, *3*, 3544.
(48) Boudreault, P.-L.; Arseneault, M.; Otis, F.; Voyer, N. *Chem. Commun.* **2008**, 2118.
(49) Smith, B. A.; Daschbach, M. M.; Gammon, S. T.; Xiao, S.; Chapman, S. E.; Hudson, C.; Suckow, M.; Piwnica-Worms, D.; Gokel, G. W.; Leevy, W. M. *Chem. Commun.* **2011**, *47*, 7977.
(50) Busschaert, N.; Wenzel, M.; Light, M. E.; Iglesias-Hernández, P.; Pérez-Tomás, R.; Gale, P. A. *J. Am. Chem. Soc.* **2011**, *133*, 14136.
(51) Moore, S. J.; Wenzel, M.; Light, M. E.; Morley, R.; Bradberry, S. J.; Gomez-Iglesias, P.; Soto-Cerrato, V.; Perez-Tomas, R.; Gale, P. A. *Chem. Sci.* **2012**, *3*, 2501.
(52) Moore, S. J.; Haynes, C. J. E.; Gonzalez, J.; Sutton, J. L.; Brooks, S. J.; Light, M. E.; Herniman, J.; Langley, G. J.; Soto-Cerrato, V.; Perez-Tomas, R.; Marques, I.; Costa, P. J.; Felix, V.; Gale, P. A. *Chem. Sci.* **2013**, *4*, 103.
(53) Ko, S.-K.; Kim, S. K.; Share, A.; Lynch, V. M.; Park, J.; Namkung, W.; Van Rossom, W.; Busschaert, N.; Gale, P. A.; Sessler, J. L.; Shin, I. *Nat. Chem.* **2014**, *6*, 885.
(54) Soto-Cerrato, V.; Manuel-Manresa, P.; Hernando, E.; Calabuig-Fariñas, S.; Martinez-Romero, A.; Fernandez Dueñas, V.; Sahlholm, K.; Knopfel, T.; Garcia-Valverde, M.; Rodilla, A. M.; Jantus-Lewintre, E.; Farras, R.; Ciruela, F.; Perez-Tomas, R.; Quesada, R. *J. Am. Chem. Soc.* **2015**, *137*, 15892.
(55) Saha, T.; Hossain, M. S.; Saha, D.; Lahiri, M.; Talukdar, P. *J. Am. Chem. Soc.* **2016**, *138*, 7558.
(56) Saggiomo, V.; Otto, S.; Marques, I.; Felix, V.; Torroba, T.; Quesada, R. *Chem. Commun.* **2012**, *48*, 5274.
(57) Haynes, C. J. E.; Moore, S. J.; Hiscock, J. R.; Marques, I.; Costa, P. J.; Felix, V.; Gale, P. A. *Chem. Sci.* **2012**, *3*, 1436.
(58) Busschaert, N.; Bradberry, S. J.; Wenzel, M.; Haynes, C. J. E.; Hiscock, J. R.; Kirby, I. L.; Karagiannidis, L. E.; Moore, S. J.; Wells, N. J.; Herniman, J.; Langley, G. J.; Horton, P. N.; Light, M. E.; Marques, I.; Costa, P. J.; Felix, V.; Frey, J. G.; Gale, P. A. *Chem. Sci.* **2013**, *4*, 3036.
(59) Lipinski, C. A.; Lombardo, F.; Dominy, B. W.; Feeney, P. J. *Adv. Drug Delivery Rev.* **1997**, *23*, 3.
(60) *Marvin 5.8.0*, 2012; ChemAxon (http://www.chemaxon.com).
(61) Deshmukh, S. C.; Roy, A.; Talukdar, P. *Org. Biomol. Chem.* **2012**, *10*, 7536.
(62) Deshmukh, S. C.; Talukdar, P. *J. Org. Chem.* **2014**, *79*, 11215.
(63) Saha, T.; Dasari, S.; Tewari, D.; Prathap, A.; Sureshan, K. M.; Bera, A. K.; Mukherjee, A.; Talukdar, P. *J. Am. Chem. Soc.* **2014**, *136*, 14128.
(64) Sugisaki, C. H.; Ruland, Y.; Baltas, M. *Eur. J. Org. Chem.* **2003**, *2003*, 672.
(65) Saha, T.; Roy, A.; Gening, M. L.; Titov, D. V.; Gerbst, A. G.; Tsvetkov, Y. E.; Nifantiev, N. E.; Talukdar, P. *Chem. Commun.* **2014**, *50*, 5514.
(66) Roy, A.; Saha, T.; Gening, M. L.; Titov, D. V.; Gerbst, A. G.; Tsvetkov, Y. E.; Nifantiev, N. E.; Talukdar, P. *Chem. - Eur. J.* **2015**, *21*, 17445.
(67) Benz, R.; McLaughlin, S. *Biophys. J.* **1983**, *41*, 381.
(68) Biwersi, J.; Tulk, B.; Verkman, A. S. *Anal. Biochem.* **1994**, *219*, 139.
(69) Frisch, M. J.; Trucks, G. W.; Schlegel, H. B.; Scuseria, G. E.; Robb, M. A.; Cheeseman, J. R.; Scalmani, G.; Barone, V.; Mennucci, B.; Petersson, G. A.; Nakatsuji, H.; Caricato, M.; Li, X.; Hratchian, H. P.; Izmaylov, A. F.; Bloino, J.; Zheng, G.; Sonnenberg, J. L.; Hada, M.; Ehara, M.; Toyota, K.; Fukuda, R.; Hasegawa, J.; Ishida, M.; Nakajima, T.; Honda, Y.; Kitao, O.; Nakai, H.; Vreven, T.; Montgomery, J. A., Jr.; Peralta, J. E.; Ogliaro, F.; Bearpark, M.; Heyd, J. J.; Brothers, E.; Kudin, K. N.; Staroverov, V. N.; Keith, T.; Kobayashi, R.; Normand, J.; Raghavachari, K.; Rendell, A.; Burant, J. C.; Iyengar, S. S.; Tomasi, J.; Cossi, M.; Rega, N.; Millam, J. M.; Klene, M.; Knox, J. E.; Cross, J. B.; Bakken, V.; Adamo, C.; Jaramillo, J.; Gomperts, R.; Stratmann, R. E.; Yazyev, O.; Austin, A. J.; Cammi, R.; Pomelli, C.; Ochterski, J. W.; Martin, R. L.; Morokuma, K.; Zakrzewski, V. G.; Voth, G. A.; Salvador, P.; Dannenberg, J. J.; Dapprich, S.; Daniels, A. D.; Farkas, O.; Foresman, J. B.; Ortiz, J. V.; Cioslowski, J.; Fox, D. J. *Gaussian 09*, revision B.01; Gaussian, Inc.: Wallingford, CT, 2010.
(70) Chai, J.-D.; Head-Gordon, M. *Phys. Chem. Chem. Phys.* **2008**, *10*, 6615.
(71) Stewart, J. J. P. *MOPAC2012*, Stewart Computational Chemistry: Colorado Springs, CO, 2012.
(72) Korth, M. *J. Chem. Theory Comput.* **2010**, *6*, 3808.
(73) Verkman, A. S. *Am. J. Physiol. Cell Physiol.* **1990**, *259*, C375.
(74) Zhu, Y.; Parsons, S. P.; Huizinga, J. D. *Neurogastroenterol. Motil.* **2010**, *22*, 704.
(75) Tsukimoto, M.; Harada, H.; Ikari, A.; Takagi, K. *J. Biol. Chem.* **2005**, *280*, 2653.
(76) Yu, L.; Jiang, X. H.; Zhou, Z.; Tsang, L. L.; Yu, M. K.; Chung, Y. W.; Zhang, X. H.; Wang, A. M.; Tang, H.; Chan, H. C. *PLoS One* **2011**, *6*, e17322.
(77) Ly, J. D.; Grubb, D. R.; Lawen, A. *Apoptosis* **2003**, *8*, 115.
(78) Chu, Z.-L.; Pio, F.; Xie, Z.; Welsh, K.; Krajewska, M.; Krajewski, S.; Godzik, A.; Reed, J. C. *J. Biol. Chem.* **2001**, *276*, 9239.
(79) Druškovič, M.; Šuput, D.; Milisav, I. *Croatian Med. J.* **2006**, *47*, 832.
(80) Ashkenazi, A. *Nat. Rev. Drug Discovery* **2008**, *7*, 1001.
(81) Loreto, C.; La Rocca, G.; Anzalone, R.; Caltabiano, R.; Vespasiani, G.; Castorina, S.; Ralph, D. J.; Cellek, S.; Musumeci, G.; Giunta, S.; Djinovic, R.; Basic, D.; Sansalone, S. *BioMed Res. Int.* **2014**, *2014*, 616149.
(82) Smiley, S. T.; Reers, M.; Mottola-Hartshorn, C.; Lin, M.; Chen, A.; Smith, T. W.; Steele, G. D.; Chen, L. B. *Proc. Natl. Acad. Sci. U. S. A.* **1991**, *88*, 3671.
(83) Cossarizza, A.; Baccaranicontri, M.; Kalashnikova, G.; Franceschi, C. *Biochem. Biophys. Res. Commun.* **1993**, *197*, 40.

DOI: 10.1021/jacs.6b10379
J. Am. Chem. Soc. 2016, 138, 16443−16451

(84) Sabharwal, S. S.; Schumacker, P. T. *Nat. Rev. Cancer* **2014**, *14*, 709.
(85) Sena, L. A.; Chandel, N. S. *Mol. Cell* **2012**, *48*, 158.
(86) Liu, X.; Kim, C. N.; Yang, J.; Jemmerson, R.; Wang, X. *Cell* **1996**, *86*, 147.
(87) Li, P.; Nijhawan, D.; Budihardjo, I.; Srinivasula, S. M.; Ahmad, M.; Alnemri, E. S.; Wang, X. *Cell* **1997**, *91*, 479.
(88) Jiang, X.; Wang, X. *Annu. Rev. Biochem.* **2004**, *73*, 87.
(89) Herrera, B.; Álvarez, A. M.; Sánchez, A.; Fernández, M.; Roncero, C.; Benito, M.; Fabregat, I. *FASEB J.* **2001**, *15*, 741.
(90) Madesh, M.; Hajnoczky, G. *J. Cell Biol.* **2001**, *155*, 1003.
(91) Skulachev, V. P. *Apoptosis* **2006**, *11*, 473.
(92) Cook, S. A.; Sugden, P. H.; Clerk, A. *Circ. Res.* **1999**, *85*, 940.
(93) Tsujimoto, Y.; Shimizu, S. *Apoptosis* **2007**, *12*, 835.
(94) Cullen, S. P.; Martin, S. J. *Cell Death Differ.* **2009**, *16*, 935.
(95) Wu, J.; Liu, T.; Xie, J.; Xin, F.; Guo, L. *Cell. Mol. Life Sci.* **2006**, *63*, 949.
(96) McIlwain, D. R.; Berger, T.; Mak, T. W. *Cold Spring Harbor Perspect. Biol.* **2013**, *5*, a008656.
(97) Boulares, A. H.; Yakovlev, A. G.; Ivanova, V.; Stoica, B. A.; Wang, G.; Iyer, S.; Smulson, M. *J. Biol. Chem.* **1999**, *274*, 22932.
(98) Park, S.-H.; Choi, Y. P.; Park, J.; Share, A.; Francesconi, O.; Nativi, C.; Namkung, W.; Sessler, J. L.; Roelens, S.; Shin, I. *Chem. Sci.* **2015**, *6*, 7284.
(99) Curtin, N. J. *Nat. Rev. Cancer* **2012**, *12*, 801.
(100) Milczarek, G. J.; Martinez, J.; Bowden, G. T. *Life Sci.* **1996**, *60*, 1.
(101) Haupt, S.; Berger, M.; Goldberg, Z.; Haupt, Y. *J. Cell Sci.* **2003**, *116*, 4077.
(102) Ekert, P. G.; Silke, J.; Vaux, D. L. *Cell Death Differ.* **1999**, *6*, 1081.
(103) Shah, N.; Asch, R. J.; Lysholm, A. S.; LeBien, T. W. *Blood* **2004**, *104*, 2873.

DOI: 10.1021/jacs.6b10379
J. Am. Chem. Soc. 2016, 138, 16443−16451